Revisiting Censoring in Energy Harvesting Wireless Sensor Networks

Sayan Sen Gupta and Neelesh B. Mehta, *Senior Member, IEEE*

***Abstract*— Censoring improves the lifetime of conventional wireless sensor networks (WSNs) by reducing the number of sensor node transmissions. However, this comes at the expense of performance since measurements from fewer nodes are available. We show that in energy harvesting (EH) WSNs, in which the sensor nodes harvest energy from the environment, this trade-off is fundamentally different. For a general model in which the nodes experience independent and non-identical fading and the EH process at a node is stationary and ergodic, we derive a lower bound on the mean squared error (MSE). It leads to an insightful and explicit characterization of the optimum censoring threshold for each node. We show that it is the point at which the probability that an EH node has sufficient energy to transmit becomes 1. We also analyze the MSE outage probability, which is an alternate and widely used performance measure, which characterizes the impact of channel fading.**

I. Introduction

Lifetime is a critical issue in the design of wireless sensor networks (WSNs), which are being increasingly used in applications such as environmental monitoring, military surveillance, and healthcare due to their low cost and ease of deployment. Several lifetime improvement techniques have been explored in the literature [1]. These include clustering [2], data correlation [3], beamforming [4], and opportunistic transmission [5]. Censoring [6] is a widely studied opportunistic transmission scheme, in which each node computes a local metric and its decision to transmit depends on it. The likelihood ratio of a node's observation is used as the metric in the detection problem considered in [7]. In estimation problems, a node's measurement is the metric in [8] and a node's channel power gain is the metric in [9].

Energy harvesting (EH) is a green, alternate solution that eliminates the problem of limited lifetime in WSNs. In it, the nodes are equipped with rechargeable batteries and an EH circuitry that enables them to harvest energy from renewable sources, such as solar, vibration, and wind, and replenish their energy buffers. However, since the energy available is random, the nodes can occasionally be unavailable due to lack of energy, which affects performance.

Estimation by EH WSNs has been investigated by several papers in the literature [10]–[12]. In [13], the goal is to minimize the mean squared error (MSE) by optimizing the transmit power of an EH node in each slot depending on whether the energy arrivals in the future are known non-causally or not. The optimal power allocation problem is modeled using finite and infinite horizon Markov decision processes and solved using dynamic programming in [14]. The solution proposed in [15] determines which node should transmit in a slot and its transmit power so as to minimize the MSE over a finite time horizon; the energy arrivals are assumed to be known a priori.

The focus in the literature has primarily been on determining the transmit power of the sensor nodes. However, the efficacy of classical energy-conserving schemes, such as censoring, in EH WSNs has not been well studied. Furthermore, the fixed transmit power model, which addresses the important issue of energy-efficient power-amplifiers in sensor nodes [16], has not been well investigated. We endeavor to bridge this gap in this work. Our work brings out several new insights about how the design of EH WSNs differs from that of conventional WSNs. In conventional WSNs, increasing the censoring threshold reduces the average number of times a node transmits its observations to the fusion node (FN). Doing so increases lifetime, but it also increases the MSE. However, as we show, this monotone relationship no longer holds in EH WSNs.

A. Focus and Contributions

We analyze and optimize the performance of channel-based censoring for an EH WSN. Our contributions are as follows:

- We derive a tractable and insightful lower bound on the MSE and then provide an explicit characterization of the optimal censoring thresholds for each node that jointly minimize the bound. We show that the optimum censoring threshold for an EH node is the point where the node transitions from being energy constrained to being energy unconstrained. Here, an EH node is said to be energy unconstrained if it has sufficient energy to transmit its observation to the FN in a slot with probability 1. Else, it is said to be energy constrained.
- We also derive an upper bound on the MSE outage probability, which is the probability that the instantaneous MSE exceeds a threshold. It is an alternate and widely studied performance measure, which characterizes the impact of channel fading.

The above results are general in the following two respects. First, they apply to the general class of stationary and ergodic EH processes, which includes the widely used independent and identically distributed (i.i.d.) [10], Bernoulli [17], and Markovian EH models [13], [14]. Second, they apply to the

S. Sen Gupta and N. B. Mehta are with the Dept. of Electrical Communication Eng. (ECE), Indian Institute of Science (IISc), Bangalore, India.
Emails: sayan.riju88@gmail.com, neeleshbmehta@gmail.com

This work was partially supported by the DST-Swaranajayanti Fellowship award DST/SJF/ETA-01/2014-15.

978-1-5386-4727-1/18/$31.00 ©2018 IEEE

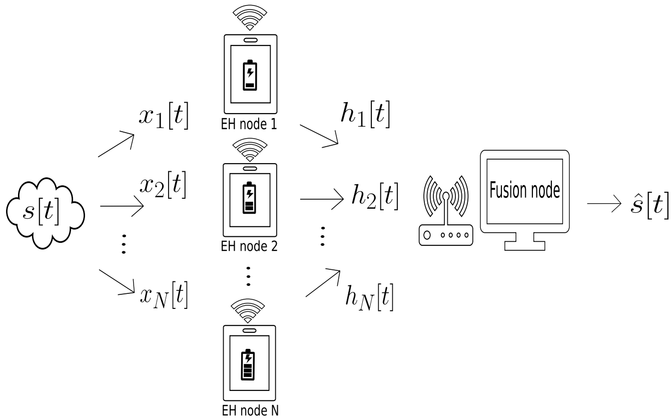

Fig. 1. An EH WSN consisting of N EH nodes that observe an unknown parameter $s[t]$ and subsequently transmit their readings to an FN, which generates an estimate $\hat{s}[t]$ of $s[t]$.

general, practically relevant case where the nodes experience statistically non-identical fading. This happens, for example, when they are at different distances from the FN.

B. Organization and Notations

This paper is organized as follows. Section II presents the system model. Section III analyzes the MSE and MSE outage probability of censoring. Simulation results are presented in Section IV, and are followed by conclusions in Section V.

Notations: The probability of an event A is denoted by $\Pr[A]$. The conditional probability of A given event B is denoted by $\Pr[A|B]$. The joint probability of A and B is denoted by $\Pr[A, B]$. For a random variable (RV) X, its probability density function (PDF) is denoted by $f_X(\cdot)$ and its expectation by $\mathbb{E}_X[\cdot]$. Similarly, the expectation conditioned on an event A is denoted by $\mathbb{E}_X[\cdot|A]$. The notation $X \sim \mathrm{CN}(\sigma^2)$ means that X is a zero-mean, circularly symmetric complex Gaussian RV with variance σ^2. For a set $\mathcal{B}$, $|\mathcal{B}|$ denotes its cardinality and $\mathcal{B}^c$ its complement. For a complex number c, c^* and $|c|$ denote its complex conjugate and absolute value, respectively. The indicator function $1_{\{a\}}$ equals 1 if a is true and is 0 otherwise.

II. System Model

We consider a time-slotted EH WSN that consists of a set $\mathcal{N} = \{1, 2, \ldots, N\}$ of EH nodes and an FN. Fig. 1 shows the system model. The models for sensor readings, EH and storage, channel fading, transmission, and reception are as follows.

Sensor Readings: The observation $x_i[t]$ at node i in slot t is given by

$$x_i[t] = s[t] + v_i[t], \quad \text{for } 1 \le i \le N, \tag{1}$$

where $s[t]$ is the parameter to be estimated in time slot t. It has a mean of zero, a variance of σ_s^2, and is i.i.d. across t. The observation noise $v_i[t] \sim \mathrm{CN}(\sigma_v^2)$ is independent of $s[t]$ and is i.i.d. across i and t.

EH and Storage Model: The EH process at a node is assumed to be stationary and ergodic with mean $\bar{H} > 0$ per slot, and is i.i.d. across nodes. The energy is harvested at the beginning of a slot and is stored in an energy buffer for use in that slot and subsequent slots. The buffer capacity is taken to be infinite to ensure analytical tractability [10], [13], [15].

Channel Model: Let $h_i[t]$ be the channel power gain between node i and the FN in time slot t. It is an exponential RV with mean λ_i, which models Rayleigh fading. We assume a block fading model in which the channel fades of a node are i.i.d. across time and are independent across nodes. Different nodes can have different mean channel power gains. We also assume that the EH and the channel fading processes are mutually independent [14]. Let $\mathbf{h}(t) = (h_1(t), \ldots, h_N(t))$.

Transmission and Censoring Scheme: The nodes amplify and forward their observations to the FN over a set of orthogonal channels.[1] Each node uses a fixed transmit power P. The energy consumed by the node to transmit its observations to the FN is PT_{tx}, where T_{tx} is the transmission duration. Let

$$\rho = \frac{\bar{H}}{PT_{\text{tx}}}. \tag{2}$$

A node is said to be *active* in a slot if it has sufficient energy to transmit, else it is *inactive*. Only an active node can transmit in a slot.

In a slot, node i first checks if its channel power gain exceeds a censoring threshold θ_i. If so, it transmits if it is active. Let $\boldsymbol{\theta} = (\theta_1, \ldots, \theta_N)$ denote the censoring vector.

Reception Model: The signal received by the FN from node i in slot t is given by

$$y_i[t] = \sqrt{\alpha h_i[t]} x_i[t] \, e^{j\phi_i[t]} + w_i[t], \quad \text{for } 1 \le i \le N, \tag{3}$$

where $\alpha = \frac{P}{\sigma_s^2 + \sigma_v^2}$, $\phi_i[t]$ is the phase of the i^{th} channel, and $w_i[t] \sim \mathrm{CN}(\sigma_w^2)$ is the noise at the receiver for the i^{th} channel in time slot t. The noise at the receiver is i.i.d. across nodes and slots. Since the signal, noise, channel fading, and EH processes are stationary, we drop the time parameter t henceforth. Let $\mathcal{T}$ denote the set of nodes that transmit in a slot.

Estimation at the FN: Based on the received signal vector, the FN computes a linear minimum mean squared error (LMMSE) estimate of s based on its knowledge of h_i, for $i \in \mathcal{T}$, and the first and second order statistics of the signal and noise [18, Chap. IV]. The instantaneous MSE, which averages over the signal and noise but not the channel fading, is denoted as $\mathsf{MSE}(\mathcal{T})$. It is given by [18, Chap. IV]

$$\begin{aligned} \mathsf{MSE}(\mathcal{T}) &= \mathbb{E}_{s,\hat{s}}\left[|s - \hat{s}|^2 \,\middle|\, \mathcal{T} \right], \\ &= \left(\sigma_v^{-2} \sum_{i \in \mathcal{T}} \frac{h_i}{h_i + \frac{\sigma_w^2 (\sigma_s^2 + \sigma_v^2)}{\sigma_v^2 P}} + \sigma_s^{-2} \right)^{-1}. \end{aligned} \tag{4}$$

[1]We do not consider the alternate model in which all nodes transmit simultaneously over the same channel, such that their signals combine coherently at the FN. This model requires tight synchronization between sensor nodes and the FN, and is difficult to realize in practice in WSNs. Furthermore, the orthogonal channel model is justified when the WSN is not bandwidth-constrained.

III. Performance Analysis

Let A_i be the event that node i is active, S_i be the event that node i is selected, and T_i be the event that node i transmits.

A. MSE Analysis

From (4), the average MSE, which is denoted by $\overline{\mathsf{MSE}}$, is

$$\overline{\mathsf{MSE}} = \sum_{\mathcal{T} \subseteq \mathcal{N}} \mathbb{E}_{\mathbf{h}} \left[\left(\sigma_v^{-2} \sum_{i \in \mathcal{T}} \frac{h_i}{h_i + \frac{\sigma_w^2 (\sigma_s^2 + \sigma_v^2)}{\sigma_v^2 P}} + \sigma_s^{-2} \right)^{-1} \middle| \mathcal{T} \right] \times \Pr[\mathcal{T}]. \quad (5)$$

Evaluating (5) is analytically intractable. We, therefore, derive an insightful lower bound for it. Let $\Pr[\mathrm{A}_i] = \zeta_i$. Node i is said to be *energy unconstrained* if $\zeta_i = 1$. Else, it is *energy constrained*.

Lemma *1:* Node i is energy constrained if

$$\theta_i < -\lambda_i \log \rho, \quad (6)$$

and is energy unconstrained otherwise. Furthermore, the probability $\Pr[\mathrm{T}_i]$ that node i transmits is given by

$$\Pr[\mathrm{T}_i] = \begin{cases} \rho, & \text{if } \theta_i < -\lambda_i \log \rho, \\ e^{-\frac{\theta_i}{\lambda_i}}, & \text{else.} \end{cases} \quad (7)$$

Proof: The proof is given in Appendix A. ■

We see that as θ_i increases, i.e., as node i is censored more, its energy usage reduces, and it eventually becomes energy unconstrained.

Result *1:* Let $\mathcal{C}$ be the set of energy constrained nodes and $\mathcal{U}$ be the set of energy unconstrained nodes, as determined from Lemma 1. Then,

$$\overline{\mathsf{MSE}} \geq \Upsilon, \quad (8)$$

where

$$\Upsilon = \left(\sigma_v^{-2} \sum_{i \in \mathcal{C}} m(\theta_i, \lambda_i)\, \rho + \sigma_v^{-2} \sum_{j \in \mathcal{U}} m(\theta_j, \lambda_j)\, e^{-\frac{\theta_j}{\lambda_j}} + \sigma_s^{-2} \right)^{-1}, \quad (9)$$

and

$$m(\theta, \lambda) = \frac{1}{\lambda} \int_{\theta}^{\infty} \frac{x\ e^{-\frac{1}{\lambda}(x-\theta)}}{x + \frac{\sigma_w^2 (\sigma_s^2 + \sigma_v^2)}{\sigma_v^2 P}}\, dx. \quad (10)$$

Proof: The proof is given in Appendix B. ■

$m(\theta, \lambda)$ in (10) is easily evaluated numerically. The optimal censoring vector is as follows.

Result *2:* The optimal censoring vector $\boldsymbol{\theta}_{\mathrm{LB}}^*$ that minimizes Υ is

$$\boldsymbol{\theta}_{\mathrm{LB}}^* = (-\lambda_1 \log \rho, -\lambda_2 \log \rho, \ldots, -\lambda_N \log \rho). \quad (11)$$

Proof: The proof is given in Appendix C. ■

Remark 1: From Result 2 and Lemma 1, we see that at $\boldsymbol{\theta}_{\mathrm{LB}}^*$, each node becomes energy unconstrained. Furthermore, the optimal censoring thresholds for different nodes are different.

1) Insights from I.I.D. Case: When the channel fading processes of the nodes are statistically identical, $\lambda_1 = \cdots = \lambda_N = \lambda$ and $\theta_1 = \cdots = \theta_N = \theta$. From Results 1 and 2, the following corollary follows.

Corollary *1:* The $\overline{\mathsf{MSE}}$ lower bound in (9) simplifies to

$$\Upsilon = \begin{cases} \left(\frac{N\rho}{\sigma_v^2} m(\theta, \lambda) + \frac{1}{\sigma_s^2} \right)^{-1}, & \text{if } \theta < -\lambda \log \rho, \\ \left(\frac{N e^{-\frac{\theta}{\lambda}}}{\sigma_v^2} m(\theta, \lambda) + \frac{1}{\sigma_s^2} \right)^{-1}, & \text{else,} \end{cases} \quad (12)$$

and $\boldsymbol{\theta}_{\mathrm{LB}}^* = (-\lambda \log \rho, \ldots, -\lambda \log \rho)$.

B. MSE Outage Probability Analysis

The MSE outage probability $P_{\text{out}}(D_0)$ is given by

$$P_{\text{out}}(D_0) = \sum_{\mathcal{T} \subseteq \mathcal{N}} \Pr\Big[\mathsf{MSE}(\mathcal{T}) > D_0 \,\Big|\, \mathcal{T} \Big] \Pr[\mathcal{T}], \quad (13)$$

where D_0 is a predefined distortion threshold. An exact expression for (13) is analytically intractable. We instead obtain the following upper bound.

Result *3:* $P_{\text{out}}(D_0) \leq \Psi$, where

$$\Psi = \sum_{\mathcal{T} \subseteq \mathcal{N}} \left[\min_{z>0} \left\{ e^{z\sigma_v^2 \left(\frac{\sigma_s^2 - D_0}{\sigma_s^2 D_0} \right)} \prod_{i \in \mathcal{T}} q(\theta_i, \lambda_i, z) \right\} \right] \Pr[\mathcal{T}]. \quad (14)$$

Here,

$$q(\theta_i, \lambda_i, z) = \frac{e^{\frac{\theta_i}{\lambda_i}}}{\lambda_i} \int_{\theta_i}^{\infty} e^{-\left(\frac{z x \sigma_v^2 P}{\sigma_v^2 P x + \sigma_w^2 (\sigma_s^2 + \sigma_v^2)} + \frac{x}{\lambda_i} \right)} dx, \quad (15)$$

$$\Pr[\mathcal{T}] = \rho^{|\mathcal{T} \cap \mathcal{C}|} (1-\rho)^{|\mathcal{T}^c \cap \mathcal{C}|} \times \left[\prod_{j \in \mathcal{T} \cap \mathcal{U}} e^{-\frac{\theta_j}{\lambda_j}} \prod_{l \in \mathcal{T}^c \cap \mathcal{U}} \left(1 - e^{-\frac{\theta_l}{\lambda_l}} \right) \right]. \quad (16)$$

Proof: The proof is given in Appendix D. ■

Recall that $\mathcal{C}$ is the set of energy constrained nodes and $\mathcal{U}$ is the set of energy unconstrained nodes. The expression $\min_{z>0} \left\{ e^{z\sigma_v^2 \left(\frac{\sigma_s^2 - D_0}{\sigma_s^2 D_0} \right)} \prod_{i \in \mathcal{T}} q(\theta_i, \lambda_i, z) \right\}$ is evaluated numerically, e.g., using the `fmincon` function of Matlab. This can be avoided by choosing a specific value of z. It also yields an upper bound, which is weaker than Ψ. While a proof that $\boldsymbol{\theta}_{\mathrm{LB}}^*$ in (11) minimizes Ψ is an open problem, we shall observe numerically in Section IV that this is indeed the case.

1) Insights from I.I.D. Case: Ψ simplifies as follows.

Corollary *2:* The upper bound Ψ is given by

$$\Psi = \sum_{L=0}^{N} \binom{N}{L} \left[\min_{z>0} \left\{ e^{z\sigma_v^2 \left(\frac{\sigma_s^2 - D_0}{\sigma_s^2 D_0} \right)} \left(q(\theta, \lambda, z) \right)^L \right\} \right] \times \eta^L (1-\eta)^{N-L}, \quad (17)$$

where $\eta = \rho$, for $\theta < -\lambda \log \rho$, and $\eta = e^{-\frac{\theta}{\lambda}}$, else.

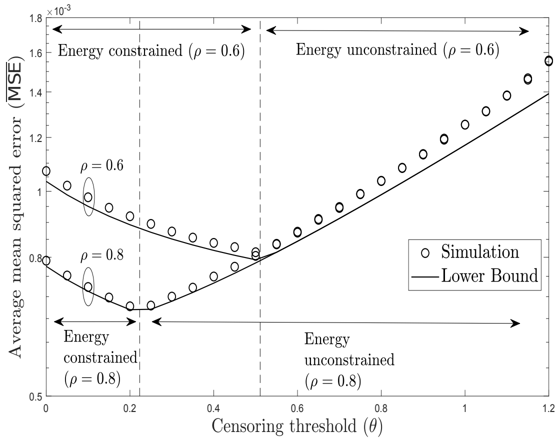

Fig. 2. $\overline{\mathsf{MSE}}$ as a function of θ for different values of ρ ($N = 30$ and $\beta = 1$).

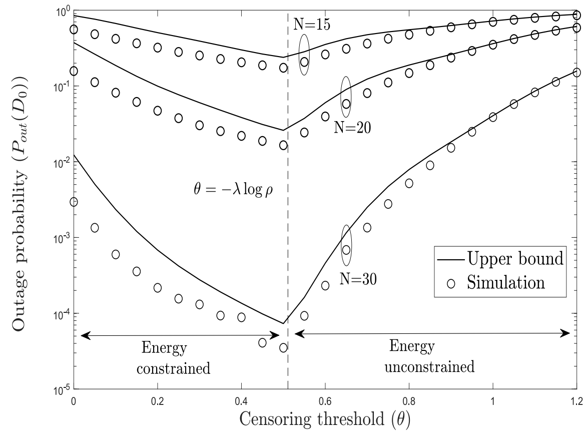

Fig. 3. $P_{\text{out}}(D_0)$ as a function of θ for different values of N ($\beta = 1, \rho = 0.6,$ and $D_0 = 0.002$).

IV. Numerical Results

We now present results from Monte Carlo simulations and compare them with our analysis. The simulations are run for a duration of 10^5 time slots in which the battery energy of each node evolves over time as per the model described in Section II. We set $P = 2$, $T_{\text{tx}} = 1$, $s \sim \text{CN}(1)$, and $\sigma_v^2 = \sigma_w^2 = 0.01$. To model independent but non-identical (i.n.i.d.) fading, we set the mean channel power gains as $\lambda_i = \beta^i$, where $\beta \leq 1$. As β decreases, the channel gains of the nodes become more statistically non-identical. The Bernoulli EH model is simulated [16].

A. I.I.D. Case

1) $\overline{\mathsf{MSE}}$: Fig. 2 plots $\overline{\mathsf{MSE}}$ as a function of the censoring threshold θ for $N = 30$ and two values of ρ, which correspond to two values of $\bar{H}$. Also plotted is the lower bound derived in (12). The lower bound tracks the simulation curve well. The censoring threshold that minimizes the lower bound is the same as the one that minimizes $\overline{\mathsf{MSE}}$. Vertical lines are drawn depicting the regions in which all the EH nodes are energy constrained and all the EH nodes are energy unconstrained. We see that as θ increases, $\overline{\mathsf{MSE}}$ decreases, which is unlike conventional WSNs. This is because as the nodes are censored more, they conserve energy and become available for transmission more often. The optimal censoring threshold lies at the boundary between the two regions. Beyond this point, $\overline{\mathsf{MSE}}$ increases because although the nodes have sufficient energy to transmit, the higher censoring threshold prevents them from being eligible for transmission. As ρ decreases, the minimum $\overline{\mathsf{MSE}}$ increases, due to less energy being harvested. Interestingly, as ρ decreases, the optimal censoring threshold increases, as can be seen from Result 2.

2) Outage: Fig. 3 plots $P_{\text{out}}(D_0)$ as a function of θ for $\rho = 0.6$ and three values of N. Also plotted is the the upper bound derived in (17). Also shown are the regions where all the nodes are energy constrained and all are unconstrained. The upper bound tracks the simulation curve well and is able to identify the optimum censoring threshold. Furthermore, it is the same as the one for $\overline{\mathsf{MSE}}$. We observe that the optimum censoring threshold does not depend on N. However, as N increases, the outage probability decreases, which is intuitive, and becomes more sensitive to the choice of the threshold.

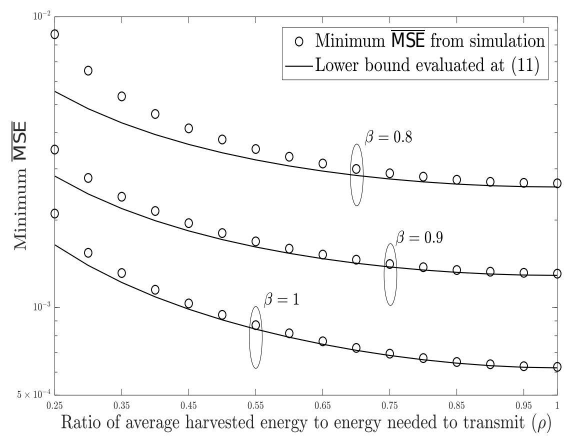

Fig. 4. Minimum $\overline{\mathsf{MSE}}$ as a function of ρ for different values of β ($N = 30$).

B. I.N.I.D. Case

1) $\overline{\mathsf{MSE}}$: Fig. 4 plots the minimum $\overline{\mathsf{MSE}}$ as a function of ρ for different values of β for $N = 30$. The minimum $\overline{\mathsf{MSE}}$ is obtained by numerically finding the optimal censoring threshold vector for each β and ρ. It turns out to be the same as that in (11). Also shown is the lower bound, in which (9) is evaluated at the censoring threshold vector given in (11). The gap between the lower bound and minimum $\overline{\mathsf{MSE}}$ decreases as ρ increases. As β decreases, the channels become weaker, which increases the minimum $\overline{\mathsf{MSE}}$. Similar to the i.i.d. case, as ρ increases, the performance improves.

2) Outage: Fig. 5 plots the minimum $P_{\text{out}}(D_0)$ as a function of ρ for different values of β and $N = 10$. As above, this minimum is found by an extensive numerical search for the

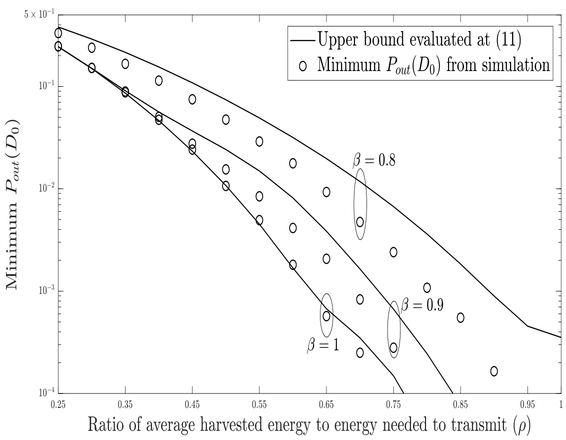

Fig. 5. Minimum $P_{\text{out}}(D_0)$ as a function of ρ for different values of β ($N = 10$ and $D_0 = 0.01$).

optimal censoring threshold vector for each value of ρ and β. As was the case for $\overline{\mathsf{MSE}}$, it turns out to be the same as that given in (11). Also shown is the upper bound, in which (14) is evaluated at the censoring threshold vector given in (11). The gap between the minimum $P_{\text{out}}(D_0)$ and the upper bound increases as ρ increases. Similar to Fig. 4, as β or ρ increase, $P_{\text{out}}(D_0)$ decreases.

V. Conclusions

We analyzed the performance of channel-based censoring for an EH WSN, in which each EH sensor node transmitted its noisy observation of a random parameter to the FN, provided that it was active and not censored. We derived bounds on $\overline{\mathsf{MSE}}$ and $P_{\text{out}}(D_0)$ of the scheme for the general class of stationary and ergodic EH processes. We saw that the optimum censoring threshold for each node that minimized $\overline{\mathsf{MSE}}$ was the same as the one that minimized the lower bound. And, it was the point where the nodes just became energy unconstrained. Numerical results showed that the MSE outage probability was also minimized at this point. Future work involves investigating the impact of imperfect channel state information and spatial correlation between the observations of different sensor nodes on the performance of such networks.

Appendix

A. Proof of Lemma 1

Let $\bar{E}_i$ be the average energy consumed by node i in a slot. Clearly, $\bar{E}_i = PT_{\text{tx}}\Pr[\mathrm{T}_i]$. A node transmits if it is active and it is not censored. Hence,

$$\Pr[\mathrm{T}_i] = \Pr[\mathrm{A}_i \cap \mathrm{S}_i]\,. \tag{18}$$

At the beginning of a slot, a node's battery energy level is a function of its channel power gains in the previous slots. As the channel fading process is independent across time and the EH and fading processes are independent of each other, $\Pr[\mathrm{A}_i \cap \mathrm{S}_i] = \Pr[\mathrm{A}_i]\Pr[\mathrm{S}_i]$. Since h_i is an exponential RV with mean λ_i, the probability that node i is not censored is given by $\Pr[\mathrm{S}_i] = \Pr[h_i > \theta_i] = e^{-\frac{\theta_i}{\lambda_i}}$. Hence, (18) becomes

$$\Pr[\mathrm{T}_i] = \zeta_i e^{-\frac{\theta_i}{\lambda_i}}. \tag{19}$$

From the law of conservation of energy, we know that

$$\bar{E}_i \leq \bar{H}. \tag{20}$$

Substituting (19) in (20) yields $PT_{\text{tx}}\zeta_i e^{-\frac{\theta_i}{\lambda_i}} \leq \bar{H}$.

Consider the following three cases:

1) When $\theta_i > -\lambda_i \log \rho$: Substituting $\rho = \frac{\bar{H}}{PT_{\text{tx}}}$ and rearranging the terms in $\theta_i > -\lambda_i \log \rho$, we get $\bar{E}_i < \bar{H}\zeta_i$.

If $\zeta_i < 1$, then $\bar{E}_i < \bar{H}$. Thus, node i accumulates an average energy of $\bar{H} - \bar{E}_i > 0$ in its battery in every slot. Hence, the energy stored in its battery will become infinite almost surely and the node is energy unconstrained. This contradicts our assumption that $\zeta_i < 1$. Hence, $\zeta_i = 1$.

2) When $\theta_i = -\lambda_i \log \rho$: Rearranging terms and substituting $\rho = \frac{\bar{H}}{PT_{\text{tx}}}$ yields $\bar{E}_i = \bar{H}\zeta_i$. As above, we can again prove that $\zeta_i = 1$.

3) When $0 \leq \theta_i < -\lambda_i \log \rho$: In this case, $\bar{E}_i > \bar{H}\zeta_i$. It is easy to see that $\zeta_i = 1$ is not possible since it violates the inequality in (20). Thus, $\zeta_i < 1$. Also, from the law of conservation of energy, we get $\bar{E}_i = \bar{H}$.

Evaluating $\Pr[T_i]$: When node i is energy unconstrained, $\zeta_i = 1$. Therefore, from (19), $\Pr[\mathrm{T}_i] = e^{-\frac{\theta_i}{\lambda_i}}$.

When node i is energy constrained, $\bar{E}_i = \bar{H}$. Rearranging terms gives $\zeta_i = \rho e^{\frac{\theta_i}{\lambda_i}}$. Substituting this in (19) yields (7).

B. Proof of Result 1

It can be shown that $\left(\sigma_v^{-2} \sum_{i \in \mathcal{T}} \frac{h_i}{h_i + \frac{\sigma_w^2(\sigma_s^2+\sigma_v^2)}{\sigma_v^2 P}} + \sigma_s^{-2}\right)^{-1}$ is a convex function of h_i, for $i \in \mathcal{T}$. For a positive-valued RV X and an event A, from Jensen's inequality, we know that $\mathbb{E}_X\left[\frac{1}{X} \,\middle|\, A\right] \geq \frac{1}{\mathbb{E}_X[X|A]}$. Hence,

$$\mathbb{E}_{\mathbf{h}}\left[\left(\sigma_v^{-2} \sum_{i \in \mathcal{T}} \frac{h_i}{h_i + \frac{\sigma_w^2(\sigma_s^2+\sigma_v^2)}{\sigma_v^2 P}} + \sigma_s^{-2}\right)^{-1} \,\middle|\, \mathcal{T}\right] \geq$$

$$\left(\sigma_v^{-2} \sum_{i \in \mathcal{T}} \mathbb{E}_{h_i}\left[\frac{h_i}{h_i + \frac{\sigma_w^2(\sigma_s^2+\sigma_v^2)}{\sigma_v^2 P}} \,\middle|\, h_i \geq \theta_i\right] + \sigma_s^{-2}\right)^{-1}. \tag{21}$$

Since h_i is an exponential RV with mean λ_i, we get

$$\mathbb{E}_{h_i}\left[\frac{h_i}{h_i + \frac{\sigma_w^2(\sigma_s^2+\sigma_v^2)}{\sigma_v^2 P}} \,\middle|\, h_i \geq \theta_i\right] = \frac{1}{\lambda_i} \int_{\theta_i}^{\infty} \frac{x\ e^{-\frac{1}{\lambda_i}(x-\theta_i)}}{x + \frac{\sigma_w^2(\sigma_s^2+\sigma_v^2)}{\sigma_v^2 P}} dx \triangleq m(\theta_i, \lambda_i)\,. \tag{22}$$

Thus, we have

$$\overline{\mathsf{MSE}} \geq \mathbb{E}_{\mathcal{T}}\left[\left(\sigma_v^{-2} \sum_{i \in \mathcal{T}} m(\theta_i, \lambda_i) + \sigma_s^{-2}\right)^{-1}\right]. \tag{23}$$

Considering all possibilities that track whether each node transmits or not, which can be written in terms of indicator functions $1_{\{\mathrm{T}_1\}}, \ldots, 1_{\{\mathrm{T}_N\}}$, (23) can be recast as

$$\overline{\mathsf{MSE}} \geq \mathbb{E}_{1_{\{\mathrm{T}_1\}},\ldots,1_{\{\mathrm{T}_N\}}}\left[\left(\sigma_v^{-2}\sum_{i=1}^{N} m(\theta_i,\lambda_i)\, 1_{\{\mathrm{T}_i\}} + \sigma_s^{-2}\right)^{-1}\right]. \tag{24}$$

From Jensen's inequality, we get

$$\overline{\mathsf{MSE}} \geq \left(\sigma_v^{-2}\sum_{i=1}^{N} m(\theta_i,\lambda_i)\,\Pr[\mathrm{T}_i] + \sigma_s^{-2}\right)^{-1}. \tag{25}$$

Substituting Lemma 1 in (25) yields the result in (9).

C. Proof of Result 2

Minimizing Υ is the same as maximizing its denominator, which is given by

$$\sigma_v^{-2}\sum_{i\in\mathcal{C}} m(\theta_i,\lambda_i)\,\rho + \sigma_v^{-2}\sum_{j\in\mathcal{U}} m(\theta_j,\lambda_j)\, e^{-\frac{\theta_j}{\lambda_j}} + \sigma_s^{-2}. \tag{26}$$

It is easy to see that

$$\max_{\theta_1,\ldots,\theta_N}\left\{\rho\sum_{i\in\mathcal{C}} m(\theta_i,\lambda_i) + \sum_{j\in\mathcal{U}} m(\theta_j,\lambda_j)\, e^{-\frac{\theta_j}{\lambda_j}}\right\} \leq$$
$$\rho\sum_{i\in\mathcal{C}}\max_{\theta_i}\{m(\theta_i,\lambda_i)\} + \sum_{j\in\mathcal{U}}\max_{\theta_j}\left\{m(\theta_j,\lambda_j)\, e^{-\frac{\theta_j}{\lambda_j}}\right\}. \tag{27}$$

It can be shown that $m(\theta_i,\lambda_i)$ is a monotonically increasing function of θ_i, for $i\in\mathcal{C}$, and $m(\theta_j,\lambda_j)\, e^{-\frac{\theta_j}{\lambda_j}}$ is a monotonically decreasing function of θ_j, for $j\in\mathcal{U}$. This implies that this upper bound in (27) is achievable and this happens when each node transitions from being energy constrained to being energy unconstrained, i.e., $\theta_i = -\lambda_i \log\rho$, for $1 \leq i \leq N$.

D. Brief Proof of Result 3

Let $P_{\text{out}}(D_0,\mathcal{T}) = \Pr[\mathsf{MSE} > D_0|\mathcal{T}]$. Utilizing (4) and performing some algebraic manipulations on $\Pr[\mathsf{MSE} > D_0|\mathcal{T}]$, we can show that

$$P_{\text{out}}(D_0,\mathcal{T}) = \Pr\left[\sum_{i\in\mathcal{T}}\frac{h_i}{h_i + \frac{\sigma_w^2(\sigma_s^2+\sigma_v^2)}{\sigma_v^2 P}} < \sigma_v^2\left(\frac{\sigma_s^2 - D_0}{\sigma_s^2 D_0}\right)\,\middle|\,\mathcal{T}\right]. \tag{28}$$

For any $z>0$, (28) can be written as

$$P_{\text{out}}(D_0,\mathcal{T}) = \Pr\left[e^{-\sum\limits_{i\in\mathcal{T}}\frac{z h_i}{h_i + \frac{\sigma_w^2(\sigma_s^2+\sigma_v^2)}{\sigma_v^2 P}}} > e^{-z\sigma_v^2\left(\frac{\sigma_s^2 - D_0}{\sigma_s^2 D_0}\right)}\,\middle|\,\mathcal{T}\right]. \tag{29}$$

Using Markov's inequality and noting that the channel power gains are i.n.i.d. exponential RVs with mean λ_i, (29) becomes

$$P_{\text{out}}(D_0,\mathcal{T}) \leq e^{z\sigma_v^2\left(\frac{\sigma_s^2 - D_0}{\sigma_s^2 D_0}\right)}\prod_{i\in\mathcal{T}} q(\theta_i,\lambda_i,z), \tag{30}$$

where $q(\theta_i,\lambda_i,z)$ is given in (15). Since (30) holds for any $z>0$, it follows that

$$P_{\text{out}}(D_0,\mathcal{T}) \leq \min_{z>0}\left\{e^{z\sigma_v^2\left(\frac{\sigma_s^2 - D_0}{\sigma_s^2 D_0}\right)}\prod_{i\in\mathcal{T}} q(\theta_i,\lambda_i,z)\right\}. \tag{31}$$

From Lemma 1 and utilizing the fact the nodes transmit independently of each other, we get

$$\Pr[\mathcal{T}] = \rho^{|\mathcal{T}\cap\mathcal{C}|}(1-\rho)^{|\mathcal{T}^c\cap\mathcal{C}|} \times\left[\prod_{j\in\mathcal{T}\cap\mathcal{U}} e^{-\frac{\theta_j}{\lambda_j}}\prod_{l\in\mathcal{T}^c\cap\mathcal{U}}\left(1 - e^{-\frac{\theta_l}{\lambda_l}}\right)\right]. \tag{32}$$

Substituting (31) and (32) in (13) gives the expression for Ψ.

References

[1] H. Yetgin, K. T. K. Cheung, M. El-Hajjar, and L. H. Hanzo, "A survey of network lifetime maximization techniques in wireless sensor networks," *IEEE Commun. Surveys Tuts.*, vol. 19, no. 2, pp. 828–854, 2nd Qtr. 2017.

[2] O. Younis, M. Krunz, and S. Ramasubramanian, "Node clustering in wireless sensor networks: recent developments and deployment challenges," *IEEE Netw.*, vol. 20, no. 3, pp. 20–25, May 2006.

[3] S. He, J. Chen, X. Li, X. Shen, and Y. Sun, "Leveraging prediction to improve the coverage of wireless sensor networks," *IEEE Trans. Parallel Distrib. Syst.*, vol. 23, no. 4, pp. 701–712, Apr. 2012.

[4] Z. Han and H. V. Poor, "Lifetime improvement of wireless sensor networks by collaborative beamforming and cooperative transmission," in *Proc. ICC*, Jun. 2007.

[5] Y. Chen and Q. Zhao, "On the lifetime of wireless sensor networks," *IEEE Commun. Lett.*, vol. 9, no. 11, pp. 976–978, Nov. 2005.

[6] S. Appadwedula, V. V. Veeravalli, and D. L. Jones, "Decentralized detection with censoring sensors," *IEEE Trans. Signal Process.*, vol. 56, no. 4, pp. 1362–1373, Apr. 2008.

[7] C. Rago, P. Willett, and Y. Bar-Shalom, "Censoring sensors: A low-communication-rate scheme for distributed detection," *IEEE Trans. Aerosp. Electron. Syst.*, vol. 32, no. 2, pp. 554–568, Apr. 1996.

[8] E. J. Msechu and G. B. Giannakis, "Sensor-centric data reduction for estimation with WSNs via censoring and quantization," *IEEE Trans. Signal Process.*, vol. 60, no. 1, pp. 400–414, Jan. 2012.

[9] J. Matamoros and C. Anton-Haro, "Opportunistic power allocation and sensor selection schemes for wireless sensor networks," *IEEE Trans. Wireless Commun.*, vol. 9, no. 2, pp. 534–539, Feb. 2010.

[10] S. Knorn, S. Dey, A. Ahlén, and D. E. Quevedo, "Distortion minimization in multi-sensor estimation using energy harvesting and energy sharing," *IEEE Trans. Signal Process.*, vol. 63, no. 11, pp. 2848–2863, Jun. 2015.

[11] S. Zhang, S. Liu, V. Sharma, and P. K. Varshney, "Optimal sensor collaboration for parameter tracking using energy harvesting sensors," *IEEE Trans. Signal Process.*, vol. 66, no. 12, pp. 3339–3353, Jun. 2018.

[12] A. Özelikkale, T. McKelvey, and M. Viberg, "Transmission strategies for remote estimation with an energy harvesting sensor," *IEEE Trans. Wireless Commun.*, vol. 16, no. 7, pp. 4390–4403, Jul. 2017.

[13] Y. Zhao, B. Chen, and R. Zhang, "Optimal power management for remote estimation with an energy harvesting sensor," *IEEE Trans. Wireless Commun.*, vol. 14, no. 11, pp. 6471–6480, Nov. 2015.

[14] M. Nourian, S. Dey, and A. Ahlén, "Distortion minimization in multi-sensor estimation with energy harvesting," *IEEE J. Sel. Areas Commun.*, vol. 33, no. 3, pp. 524–539, Mar. 2015.

[15] P. Du, Q. Yang, Z. Shen, and K. S. Kwak, "Distortion minimization in wireless sensor networks with energy harvesting," *IEEE Commun. Lett.*, vol. 21, no. 6, pp. 1393–1396, Jun. 2017.

[16] S. Rao and N. B. Mehta, "Energy harvesting WSNs for accurately estimating the maximum sensor reading: Trade-offs and optimal design," *IEEE Trans. Wireless Commun.*, vol. 14, no. 8, pp. 4562–4573, Aug. 2015.

[17] A. Kazerouni and A. Özgür, "Optimal online strategies for an energy harvesting system with Bernoulli energy recharges," in *Proc. WiOpt*, May 2015, pp. 235–242.

[18] H. V. Poor, *An Introduction to signal detection and estimation*, 2nd ed. Springer-Verlag, 1994.